

Magnetoelastic Dynamics of the Spin Jahn-Teller Transition in CoTi_2O_5

K. Guratinder,¹ R. D. Johnson^{2,3}, D. Prabhakaran,⁴ R. A. Taylor⁴, F. Lang⁴, S. J. Blundell⁴, L. S. Taran⁵, S. V. Streltsov^{5,6}, T. J. Williams⁷, S. R. Giblin⁸, T. Fennell⁹, K. Schmalzl¹⁰, and C. Stock¹

¹*School of Physics and Astronomy, University of Edinburgh, Edinburgh EH9 3JZ, United Kingdom*

²*Department of Physics and Astronomy, University College London, Gower Street, London WC1E 6BT, United Kingdom*

³*London Centre for Nanotechnology, University College London, Gordon Street, London WC1H 0AH, United Kingdom*

⁴*Department of Physics, Clarendon Laboratory, University of Oxford, Parks Road, Oxford OX1 3PU, United Kingdom*

⁵*M. N. Mikheev Institute of Metal Physics, Ural Branch of Russian Academy of Sciences, 620137 Yekaterinburg, Russia*

⁶*Institute of Physics and Technology, Ural Federal University, 620002 Yekaterinburg, Russia*

⁷*ISIS Pulsed Neutron and Muon Source, STFC Rutherford Appleton Laboratory, Harwell Campus, Didcot, Oxon OX11 0QX, United Kingdom*

⁸*School of Physics and Astronomy, Cardiff University, Cardiff CF24 3AA, United Kingdom*

⁹*Laboratory for Neutron Scattering, Paul Scherrer Institut, CH-5232 Villigen, Switzerland*

¹⁰*Juelich Centre for Neutron Science, Forschungszentrum Juelich GmbH, Outstation at Institut Laue-Langevin, Boite Postal 156, 38042 Grenoble Cedex 9, France*



(Received 20 October 2024; revised 1 April 2025; accepted 14 May 2025; published 25 June 2025)

CoTi_2O_5 has the paradox that low temperature static magnetic order is incompatible with the crystal structure owing to a mirror plane that exactly frustrates magnetic interactions. Despite no observable structural distortion with diffraction, CoTi_2O_5 does magnetically order below $T_N \sim 25$ K with the breaking of spin ground state degeneracy proposed to be a realization of the spin Jahn-Teller effect in analogy to the celebrated orbital Jahn-Teller transition. We apply neutron and Raman spectroscopy to study the dynamics of this transition in CoTi_2O_5 . We find anomalous acoustics associated with a symmetry breaking strain that characterizes the spin Jahn-Teller transition. Crucially, the energy of this phonon coincides with the energy scale of the magnetic excitations, and has the same symmetry of an optic mode, observed with Raman spectroscopy, which atypically softens in energy with decreasing temperature. Taken together, we propose that the energetics of the spin Jahn-Teller effect in CoTi_2O_5 are related to cooperative magnetoelastic fluctuations as opposed to conventional soft critical dynamics which typically drive large measurable static displacements.

DOI: [10.1103/sr9s-llly](https://doi.org/10.1103/sr9s-llly)

Structural phase transitions are typically driven by a dynamic soft mode [1–4] which freezes either continuously or discontinuously. Classic examples include soft zone center transverse optical phonons in perovskites [5–7] and zone boundary phonon anomalies that appear in orientational-like order-disorder transitions [8,9]. Such structural transitions are readily observed through diffraction techniques. However, there is a growing list of materials where a magnetostructural transition must occur based on symmetry constraints or bulk measurements, yet are not accompanied by an observable change in the Bragg peaks measured with x-ray or neutron diffraction. For example, this is the case for ferroaxial multiferroic phase transitions in $\text{RbFe}(\text{MoO}_4)_2$ [10,11], $\text{CaMn}_7\text{O}_{12}$ [12,13], and

$\text{Cu}_3\text{Nb}_2\text{O}_8$ [14,15], where changes in Bragg peaks and soft lattice dynamics are not readily observable [16]. This is despite known low temperature structural transitions derived based on symmetry constraints. A further example is certain ferroelectric metal-organic frameworks [17] which lack observable soft phonon dynamics despite known displacive ferroelectric transitions.

We address this apparent contradiction through studying the lattice and magnetic dynamics of a similar problem in the spin-Jahn Teller material CoTi_2O_5 , where a structural transition is not observable in conventional diffraction, yet must occur to allow low temperature magnetic order, which is exactly frustrated based on the high temperature nuclear structure. In analogy to the orbital Jahn-Teller theorem [18] that predicts a structural distortion will occur to break an orbital degeneracy, a similar idea has been proposed in the context of spin degeneracy from frustrated magnetism where an orbital degeneracy is absent. The “spin Jahn-Teller effect” is where a spin degeneracy drives a symmetry breaking structural transition that lifts the degeneracy of the spin manifold and facilitates long-range magnetic order.

Published by the American Physical Society under the terms of the [Creative Commons Attribution 4.0 International](https://creativecommons.org/licenses/by/4.0/) license. Further distribution of this work must maintain attribution to the author(s) and the published article's title, journal citation, and DOI.

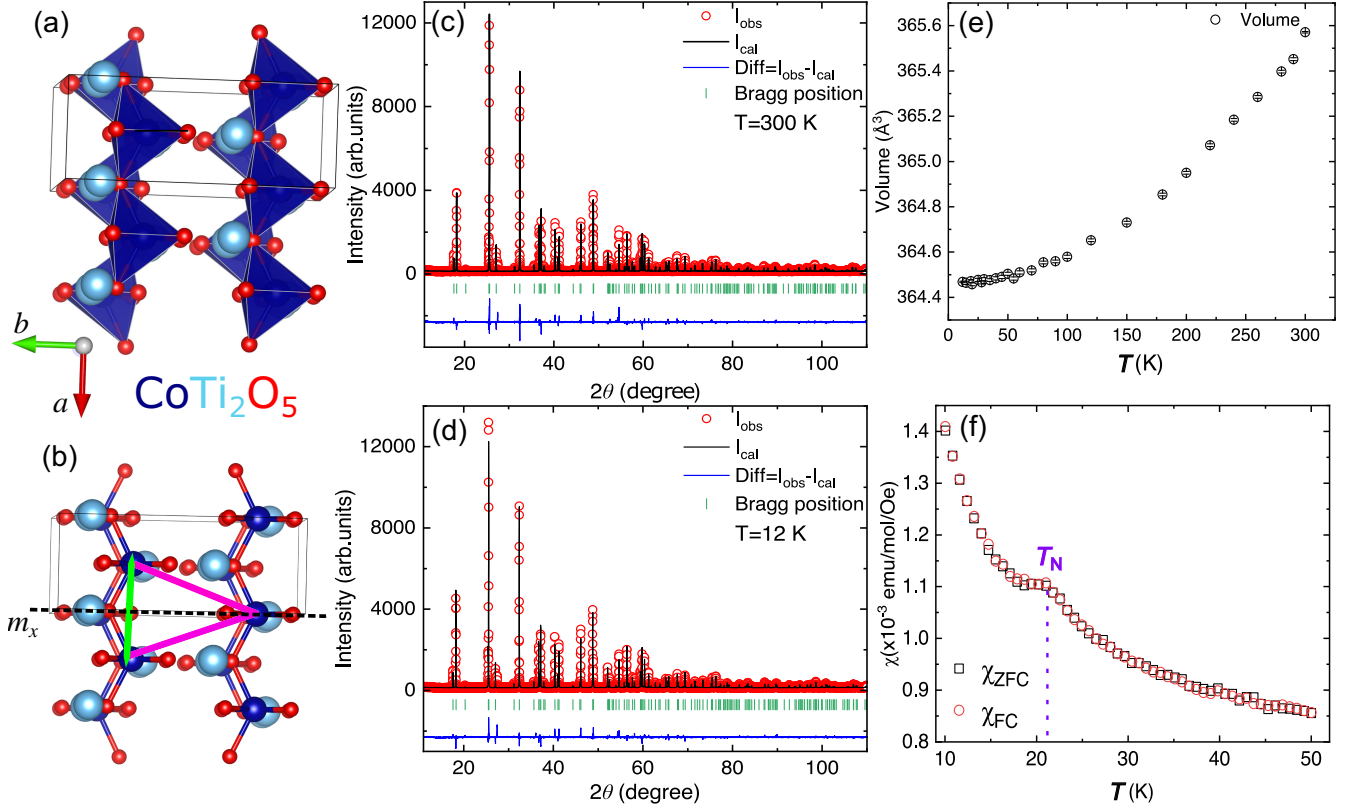


FIG. 1. Structural and magnetic properties of CoTi_2O_5 . (a),(b) The nuclear structure and the frustrating triangular arrangement of the interactions. (c),(d) The same diffraction measurements at 300 and 12 K. (e) A plot of the volume of the lattice with temperature showing no change in slope at the (f) Néel temperature of $\sim 23 \text{ K}$ measured in a powder sample with an applied field of 100 G.

Such a structural distortion originates from the competition between magnetic and elastic energy scales [19,20]. Given the reduction of the magnetic energy scales linearly with atomic positions while the elastic scales quadratically, it is favored for distortion to occur for the relief of frustrating magnetic interactions, resulting in spatially long-range magnetic order. We study the dynamics of this effect in CoTi_2O_5 by applying neutron and Raman spectroscopy. While a structural transition is not observable, we find evidence of acoustic dynamics associated with atomic displacement that is linked with magnetic frustration.

CoTi_2O_5 adopts a pseudobrookite structure with an orthorhombic space group $Cmcm$ at high temperatures [21]. The magnetic Co^{2+} ions reside on a site with $m2m(C_{2v})$ symmetry, implying that the orbital levels are already nondegenerate and therefore the normal Jahn-Teller theorem [22] discussed above does not apply. The lack of an orbital degeneracy in CoTi_2O_5 is further discussed in the Supplemental Material [23] in the context of the search for spin-orbit transitions seen in octahedrally coordinated and orbitally active Co^{2+} based compounds [24–28] which we find are absent in CoTi_2O_5 . The frustrated antiferromagnetic interactions, mediated by indirect exchange through oxygen, are illustrated in Figs. 1(a) and 1(b) and are based on exactly isosceles triangles. Because of a

crystallographic mirror plane perpendicular to $[100]$ (termed m_x), this is a perfectly frustrated geometry resulting in spin order that is expected to be unstable to thermal fluctuations. Therefore, magnetic order is not expected unless accompanied by a structural distortion (displacive and strain) [29] that transforms as the Γ_2^+ irreducible representation as identified in Ref. [30]. However, as shown in Ref. [30] applying high resolution neutron diffraction, CoTi_2O_5 does not undergo an observable structural transition yet displays spatially long-range magnetic order below $T_N \sim 25 \text{ K}$. It was therefore concluded that CoTi_2O_5 undergoes a spin Jahn-Teller transition where the structure distorts, subtly, to break the large ground state spin degeneracy imposed by the frustrating geometry. Further studies have been performed on isostructural FeTi_2O_5 and have also found similar results [31]. In the following, we investigate acoustic and optic structural dynamics near this spin Jahn-Teller transition and probe low-energy magnetic excitations that characterize low temperature magnetic order.

Neutron spectroscopy was used to study the low-energy acoustic phonons and magnetic excitations. Acoustic phonon measurements were performed on the EIGER thermal triple-axis spectrometer (PSI). High resolution magnetic spectroscopy was performed on the IN12 cold-triple axis

spectrometer (ILL). For all neutron scattering experiments, the sample was aligned such that reflections of the form $(H, K, 0)$ were within the horizontal plane. We discuss the magnetic dispersion along the $(0,0,L)$ direction in Supplemental Material [23] applying the time of flight MAPS spectrometer. The sample was grown using the traveling floating zone technique [30]. Monochromatic x-ray diffraction as a function of temperature was carried out on a Rigaku Smartlab with a Johansson monochromator and PheniX dispex. Temperature dependent Raman spectroscopy was performed to study optical phonons. Further experimental information is in Supplemental Material [23].

Figure 1 reviews the static structural and magnetic properties of CoTi_2O_5 . The nuclear structure summarized in Figs. 1(a) and 1(b) is built on chains of Co^{2+} ions along the crystallographic a axis. The chains are coupled along the crystallographic b axis via an isosceles triangular arrangement which is exactly frustrated. Monochromatic x-ray diffraction at 300 K Fig. 1(c) is compared to 12 K Fig. 1(d) with no structural distortion observed between these two temperatures (refinement and analysis discussed in Supplemental Material [23] [32,33]). This is further confirmed in Fig. 1(e), where we plot the unit cell volume as a function of temperature. At low temperatures, there is no measurable change in slope which if observed would indicate a structural distortion at T_N . However, as illustrated in Fig. 1(f), despite the frustrating geometry of the spins, a magnetic transition occurs at $T_N \sim 23$ K evidenced by a peak in the magnetic susceptibility.

We now discuss the low-energy magnetic excitations below T_N . Energy-momentum slices along K and H are shown in Figs. 2(b), 2(c), and 2(d), respectively, illustrating energetically gapped [34] magnetic excitations. Confirming expectations based on bonding in the structure and the frustrating triangular arrangement outlined above, the excitations are dispersionless along the K [Fig. 2(b)] direction and strongly dispersive along H [Figs. 2(c) and 2(d)] where Co^{2+} ions are arranged in one-dimensional chains with strong interactions along the crystallographic a axis. We note that the scans along K display two distinct magnetic modes, as expected given the presence of two magnetic ions per primitive unit cell. Fits to the low energy magnetic dispersion applying a nearest-neighbor anisotropic one-dimensional model give a coupling of 3.3 ± 0.2 meV along the chain direction, an anisotropy $D = 0.25 \pm 0.12$ meV, and less than 0.07 meV along b defined by the experimental resolution on IN12. Further measurements discussed in the Supplemental Material [23] indicate a weak 0.3 ± 0.15 meV exchange along c . The lack of any observable dispersion along the K axis in Fig. 2(b) is consistent with no measurable magnetic exchange along the crystallographic b axis. This is expected given the frustrating geometry imposed by the m_x mirror plane; however, is unexpected given the presence of low-temperature spatially long-range magnetic order.

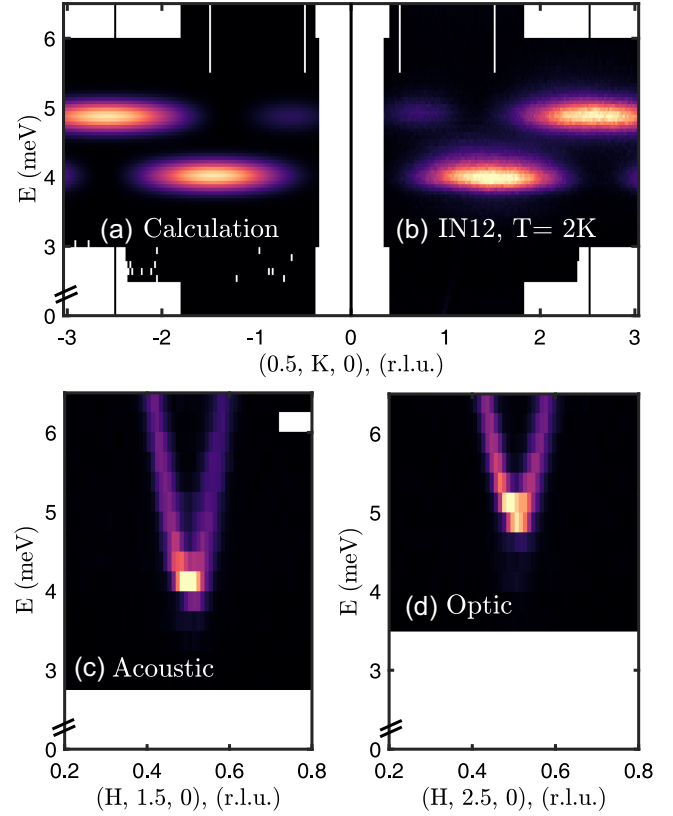


FIG. 2. The low-energy magnetic excitations in the magnetically ordered phase. Given there are two magnetic ions in the unit, there are two spin-wave branches which disperse along $(H,0,L)$ with differing phase, termed acoustic and optic here. (a) Calculated structure factors and (b) measured magnetic correlations perpendicular to the chain axis illustrating nonmeasurable dispersion indicating weak coupling. This contrasts with the resulting coupling along the chain direction displayed in (c), (d) for each of the two magnetic domains.

To understand the intensity modulation along K we compare the data to the nearest neighbor “buckled sheet” model (Supplemental Material [23], Fig. 5). Considering two Co^{2+} sites in a given a - b plane, the neutron scattering intensity from optic and acoustic correlations would take the form of $I(K) \propto [1 \pm \cos(4\pi Ky)]$, with $y \sim 0.1911$. The \pm sign fixes the relative excitation phase for the two antiferromagnetic magnon modes in the (H, L) plane with $-$ corresponding to acousticlike (in-phase) magnetic fluctuations and $+$ being opticlike with out-of-phase-like fluctuations of the neighboring spins. Figure 2(a) is a calculation to this model fixing spin excitations at 4 and 4.85 meV. Dispersive H slices for these two modes are shown in Figs. 2(c) and 2(d) (see Supplemental Material [23] for further details).

With a crystallographic distortion not observable with high resolution x-ray or neutron diffraction and no measurable dispersion of the spin excitations along b , we investigate the acoustic shear phonons in Fig. 3. Acoustic lattice fluctuations can be very sensitive to small structural

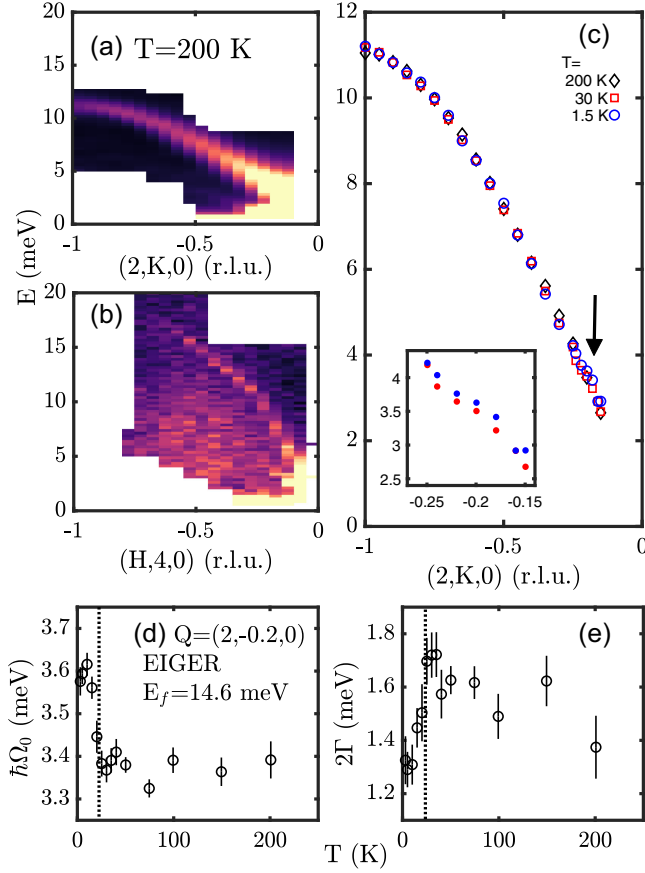


FIG. 3. Acoustic phonons in CoTi_2O_5 with the dispersion at $T = 200$ K for acoustic phonons propagating along b^* (a) and a^* (b) (note the momentum and energy broadened paramagnetic scattering near $H \sim -0.5$). An anomaly in the dispersion is evident at $\vec{Q} \sim (2, -0.2, 0)$ (c). (d) and (e) The energy position ($\hbar\Omega_0$) and full width at half maximum (2Γ) as a function of temperature.

distortions as motivated by recent studies linking low-energy acoustic phonons with weak nematic order in pnictides and chalcogenides [35,36], previous works on the dynamic Jahn-Teller effects in rare earth compounds [37–39], and also the sensitivity of acoustic phonons to orbital Jahn-Teller effects [40–46]. Figure 3(a) displays the shear mode with Γ_2^+ symmetry (B_{1g} in the notation of Ref. [47]) and Fig. 3(b) the shear mode with Γ_4^+ symmetry (B_{2g} in Ref. [47] notation). The Γ_2^+ shear mode [Fig. 3(a)] has a lower energy and is defined by a shear with unique crystallographic c axis with the correct symmetry to break the m_x mirror plane in Fig. 1(b). Given its lower energy scale and correct symmetry, we study the temperature dependence of this acoustic phonon in Fig. 3(c), noting a small anomaly in the dispersion at $K \sim -0.2$ displayed in the inset.

Figures 3(d) and 3(e) plot the energy values ($\hbar\Omega_0$) and full width (2Γ) against temperature obtained from constant $\vec{Q} = (2, -0.2, 0)$ scans fit to a damped harmonic oscillator

convolved with the experimental resolution (discussed in Supplemental Material [23]). The measured Néel transition temperature, from susceptibility, is marked by the dashed line in both panels. On cooling below T_N , there is an abrupt hardening of the acoustic phonon at this position accompanied by a sharpening in energy indicative of increased phonon lifetime. Given that in the limit $q \rightarrow 0$ the acoustic phonon velocity is related [48] to the elastic constant (in this case C_{66} [47]), the hardening of this acoustic phonon at low temperatures in the magnetically ordered phase is indicative of a dynamic strain. We suggest this is a dynamic effect as no change on this scale (5%–6%) is observed in the cell volume [49] presented in Fig. 1 or splitting of nuclear Bragg peaks on the scale reported for similar energy shifts in the acoustic phonons in other materials [50].

Having observed an anomaly in the acoustic phonons at T_N with the correct symmetry to break the frustrating m_x mirror plane, we now study the optical phonons with a single crystal sample using Raman spectroscopy. CoTi_2O_5 has 16 atoms in the primitive unit cell, giving 48 positional degrees of freedom. The Γ point, 48-dimensional atomic displacement representation, Γ_r , decomposes into the following irreducible representations; $[\Gamma_r = 8\Gamma_1^+ + 5\Gamma_2^+ + 8\Gamma_3^+ + 3\Gamma_4^+ + 3\Gamma_1^- + 8\Gamma_2^- + 5\Gamma_3^- + 8\Gamma_4^-]$. Of the 45 optic modes, 24 are Raman active (those that are parity even, as denoted by a + subscript). Polarized Raman spectroscopy was performed in reflection geometry, with incident and scattered wave vectors parallel to the c axis (Z). In this geometry only the $8\Gamma_1^+$ and $5\Gamma_2^+$ modes are excited. Furthermore, the Γ_1^+ excitations are isolated in the unrotated polarization channels $-Z(XX)Z$ and $-Z(YY)Z$ (in Porto’s notation, where $X||a$ and $Y||b$), and the Γ_2^+ excitations are isolated in the rotated $-Z(XY)Z$ and $-Z(YX)Z$ channels.

Figure 4(a) shows the Raman spectra displaying all 5 Γ_2^+ modes with the same symmetry as the anomalous acoustic mode (related to C_{66}) discussed above. The temperature dependence of select modes is presented in Figs. 4(b)–4(d). Arguably, all Γ_2^+ modes display an anomaly at T_N , however, we note these effects are less than 0.025 meV which is negligible in comparison to the energetics of the Γ_2^+ acoustic phonon and magnons discussed above. Figure 4(c) illustrates a softening with temperature of the phonon mode near 21.5 meV that contrasts with the hardening typically expected with decreasing temperature and observed for the other optical phonons (see Supplemental Material [23] for temperature dependence of all 5 Γ_2^+ modes). Phonons typically harden in energy owing to loss of anharmonic effects and lattice contraction [Fig. 1(e)], and energetic softening supports a structural instability with the same symmetry analogous to soft optic phonon driven transitions in classic perovskites [3,5]. This supports a structural instability at T_N with Γ_2^+ symmetry

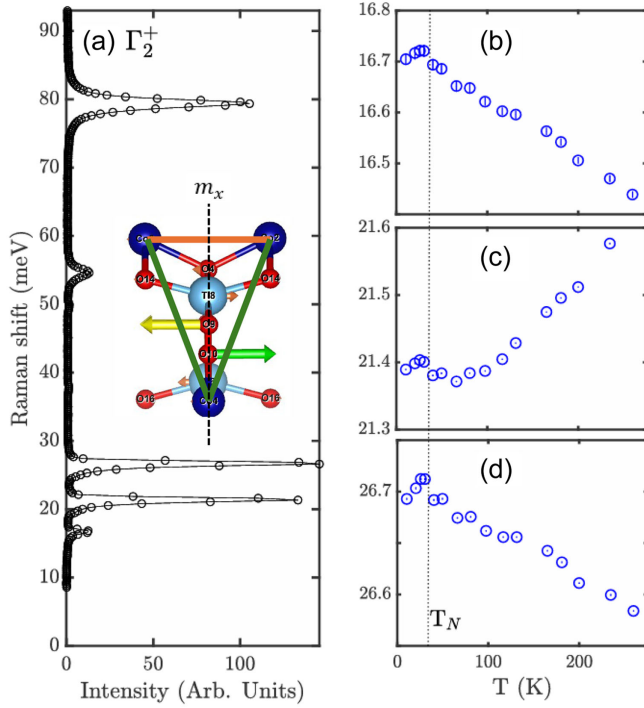


FIG. 4. (a) Raman spectra sensitive to optic phonon modes with Γ_2^+ symmetry which break the frustrating m_x mirror plane illustrated in the inset through the motion of the oxygen atoms. (b)–(d) Temperature dependence of several modes with (c) displaying a softening.

required to break the magnetic frustration outlined in Fig. 1(b).

Density functional theory was used to calculate the phonon eigenvectors and energies which were in agreement with the observed phonon mode energies (see Supplemental Material [23]) and [51–54] for parameter choices. We highlight in the inset of Fig. 4(a) the atomic displacements (eigenmode) associated with the ~ 21.5 meV mode displayed in Fig. 4(c). The displacements tied with this particular optic phonon mode move the oxygen atoms out of the mirror plane m_x . This breaks the frustration illustrated in Figs. 1(a) and 1(b). We note that the low-energy acoustic shear mode, presented above (Fig. 3), couples directly to the optic mode as it has the same Γ_2^+ symmetry [47] and importantly has the same energy as the dispersionless magnetic excitations along K . This is suggestive of magnetoelastic coupling confirmed through recent macroscopic strain measurements that are able to switch magnetic domains in this compound [55].

We observe an anomalous temperature dependence at T_N of an acoustic phonon mode with the correct symmetry to break the frustrating magnetic interactions [illustrated in Figs. 1(a) and 1(b)] in the absence of an observable structural distortion with diffraction. The energy scale of this anomaly [Fig. 3(c)] is comparable to the energy scale of the magnetic exchange $J \sim 3$ meV and T_N , while

significantly larger than the crystalline anisotropy $D \sim 0.25$ meV discussed above. This indicates a coupling between strain and magnetic order. Supporting this and as noted in Ref. [55], considering structural and magnetic order parameters (defined by δ and Φ , respectively), the lowest order invariant in the Landau expansion scales as $\sim \delta \Phi^2$ illustrating a phenomenological mechanism for coupling strain and magnetism in CoTi_2O_5 . Based on experimental and symmetry grounds, we propose that the magnetic transition in CoTi_2O_5 is dynamically driven through cooperative magnetoelastic fluctuations rather than conventional soft phonon dynamics (like in perovskites) or more exotic mechanisms such as nematic order or biquadratic exchange suggested in other triangular magnets [56–58].

In summary, we report neutron inelastic scattering results that reveal a Γ_2^+ shear phonon that hardens at T_N . Furthermore, this phonon mode has the same symmetry as an anomalous optic phonon probed with Raman spectroscopy. The Γ_2^+ acoustic shear mode energetics (in Fig. 3) coincide with those of the magnons presented in Fig. 2. The absence of a measurable static structural distortion nor a magnetic dispersion along K appears to discount a conventional magnetostructural displacive phase transition that breaks m_x . Instead, we propose that our characterization of the dynamics implies that spin Jahn-Teller physics is driven by magnetoelastic dynamics. We note that our results indicate the role of acoustic phonons in establishing the required magnetostructural coupling is at the heart of spin Jahn-Teller physics, when the acoustic phonon and magnon energetics are comparable and of the same symmetry. Our results also suggest that acoustics are a promising avenue to investigate for the study of critical dynamics of magnetostructural transitions in materials where conventional soft lattice dynamics and changes in Bragg peaks are not observable.

Acknowledgments—The work done at UoE was funded by EPSRC (EP/V03605X/1, EP/R032130/1, EP/R013004/1) and the STFC. D.P. acknowledges EPSRC Grant No. EP/T028637/1, and the Oxford-ShanghaiTech Collaboration project for financial support. Work at Cardiff was funded through EP/X034739/1. S.J.B. acknowledges support from UK Research and Innovation (UKRI) under the UK government’s Horizon Europe funding guarantee (Grant No. EP/X025861/1). D.F.T. calculations were supported by the Russian Science Foundation (Project No. RSF 23-12-00159), while their analysis by Ministry of Science and Higher Education through project Quantum.

- [1] W. Cochran, Crystal stability and the theory of ferroelectricity, *Adv. Phys.* **9**, 387 (1960).
- [2] W. Cochran, Crystal stability and the theory of ferroelectricity 2. Piezoelectric crystals, *Adv. Phys.* **10**, 401 (1961).

- [3] G. Shirane, Neutron scattering studies of structural phase transitions at Brookhaven, *Rev. Mod. Phys.* **46**, 437 (1974).
- [4] R. A. Cowley and S. M. Shapiro, Structural phase transitions, *J. Phys. Soc. Jpn.* **75**, 111001 (2006).
- [5] G. Shirane, J. D. Axe, J. Harada, and J. P. Remeika, Soft ferroelectric modes in lead titanate, *Phys. Rev. B* **2**, 155 (1970).
- [6] J. Harada, J. D. Axe, and G. Shirane, Determination of the normal vibrational displacements in several perovskites by inelastic neutron scattering, *Acta Crystallogr. Sect. A* **26**, 608 (1970).
- [7] J. Harada, J. D. Axe, and G. Shirane, Neutron-scattering study of soft modes in cubic BaTiO₃, *Phys. Rev. B* **4**, 155 (1971).
- [8] Y. Yamada, Y. Noda, J. D. Axe, and G. Shirane, Dynamical critical phenomena in ND₃Br, *Phys. Rev. B* **9**, 4429 (1974).
- [9] M. J. Harris, M. T. Dove, I. P. Swainson, and M. E. Hagen, Anomalous dynamical effects in calcite CaCO₃, *J. Phys. Condens. Matter* **10**, L423 (1998).
- [10] M. Kenzelmann, G. Lawes, A. B. Harris, G. Gasparovic, C. Broholm, A. P. Ramirez, G. A. Jorge, M. Jaime, S. Park, Q. Huang, A. Y. Shapiro, and L. A. Demianets, Direct transition from a disordered to a multiferroic phase on a triangular lattice, *Phys. Rev. Lett.* **98**, 267205 (2007).
- [11] A. J. Hearmon, F. Fabrizi, L. C. Chapon, R. D. Johnson, D. Prabhakaran, S. V. Streltsov, P. J. Brown, and P. G. Radaelli, Electric field control of the magnetic chiralities in ferroaxial multiferroic RbFe(MoO₄)₂, *Phys. Rev. Lett.* **108**, 237201 (2012).
- [12] R. D. Johnson, L. C. Chapon, D. D. Khalyavin, P. Manuel, P. G. Radaelli, and C. Martin, Giant improper ferroelectricity in the ferroaxial magnet CaMn₇O₁₂, *Phys. Rev. Lett.* **108**, 067201 (2012).
- [13] F. Kadlec, V. Goian, C. Kadlec, M. Kempa, P. c. v. Vaněk, J. Taylor, S. Rols, J. Prokleška, M. Orlita, and S. Kamba, Possible coupling between magnons and phonons in multiferroic CaMn₇O₁₂, *Phys. Rev. B* **90**, 054307 (2014).
- [14] R. D. Johnson, S. Nair, L. C. Chapon, A. Bombardi, C. Vecchini, D. Prabhakaran, A. T. Boothroyd, and P. G. Radaelli, Cu₃Nb₂O₈: A multiferroic with chiral coupling to the crystal structure, *Phys. Rev. Lett.* **107**, 137205 (2011).
- [15] N. Giles-Donovan, N. Qureshi, R. D. Johnson, L. Y. Zhang, S.-W. Cheong, S. Cochran, and C. Stock, Imitation of spin density wave order in Cu₃Nb₂O₈, *Phys. Rev. B* **102**, 024414 (2020).
- [16] S. Kamba, Soft-mode spectroscopy of ferroelectrics and multiferroics: A review, *APL Mater.* **9**, 020704 (2021).
- [17] L. Ding, C. V. Colin, V. Simonet, C. Stock, J.-B. Brubach, M. Verseils, P. Roy, V. G. Sakai, M. M. Koza, A. Piovano, A. Ivanov, J. A. Rodriguez-Rivera, S. de Brion, and M. Songvilay, Lattice dynamics and spin excitations in the metal-organic framework CH₃NH₃CoHCOO₃, *Phys. Rev. Mater.* **7**, 084405 (2023).
- [18] G. A. Gehring and K. A. Gehring, Co-operative Jahn-Teller effects, *Rep. Prog. Phys.* **38**, 1 (1975).
- [19] O. Tchernyshyov, R. Moessner, and S. L. Sondhi, Order by distortion and string modes in pyrochlore antiferromagnets, *Phys. Rev. Lett.* **88**, 067203 (2002).
- [20] Y. Yamashita and K. Ueda, Spin-driven Jahn-Teller distortion in a pyrochlore system, *Phys. Rev. Lett.* **85**, 4960 (2000).
- [21] H. Mullerbuschbaum and M. Waburg, Pseudobrookite mit weitgehend geordneter metallverteilung: CoTi₂O₅, MgTi₂O₅ und FeTi₂O₅, *Monatsch. Chem.* **114**, 21 (1983).
- [22] S. V. Streltsov and D. I. Khomskii, Jahn-Teller effect and spin-orbit coupling: Friends or foes?, *Phys. Rev. X* **10**, 031043 (2020).
- [23] See Supplemental Material at <http://link.aps.org/supplemental/10.1103/sr9s-llly> for information on experimental aspects, phonon lineshapes, magnetic dispersions indicative of coupling, and density functional theory compared with Raman.
- [24] R. A. Cowley, W. J. L. Buyers, C. Stock, Z. Yamani, C. Frost, J. W. Taylor, and D. Prabhakaran, Neutron scattering investigation of the $d-d$ excitations below the Mott gap of CoO, *Phys. Rev. B* **88**, 205117 (2013).
- [25] F. Wallington, A. M. Arevalo-Lopez, J. W. Taylor, J. R. Stewart, V. Garcia-Sakai, J. P. Attfield, and C. Stock, Spin-orbit transitions in α - and γ -CoV₂O₆, *Phys. Rev. B* **92**, 125116 (2015).
- [26] P. M. Sarte, R. A. Cowley, E. E. Rodriguez, E. Pachoud, D. Le, V. García-Sakai, J. W. Taylor, C. D. Frost, D. Prabhakaran, C. MacEwen, A. Kitada, A. J. Browne, M. Songvilay, Z. Yamani, W. J. L. Buyers, J. P. Attfield, and C. Stock, Disentangling orbital and spin exchange interactions for Co²⁺ on a rocksalt lattice, *Phys. Rev. B* **98**, 024415 (2018).
- [27] P. M. Sarte, A. M. Arévalo-López, M. Songvilay, D. Le, T. Guidi, V. García-Sakai, S. Mukhopadhyay, S. C. Capelli, W. D. Ratcliff, K. H. Hong, G. M. McNally, E. Pachoud, J. P. Attfield, and C. Stock, Ordered magnetism in the intrinsically decorated $j_{\text{eff}} = \frac{1}{2}$ α -CoV₃O₈, *Phys. Rev. B* **98**, 224410 (2018).
- [28] M. Songvilay, J. Robert, S. Petit, J. A. Rodriguez-Rivera, W. D. Ratcliff, F. Damay, V. Balédent, M. Jiménez-Ruiz, P. Lejay, E. Pachoud, A. Hadj-Azzem, V. Simonet, and C. Stock, Kitaev interactions in the Co honeycomb antiferromagnets Na₃Ca₂SbO₆ and Na₂Co₂TeO₆, *Phys. Rev. B* **102**, 224429 (2020).
- [29] C. Stock, L. C. Chapon, O. Adamopoulos, A. Lappas, M. Giot, J. W. Taylor, M. A. Green, C. M. Brown, and P. G. Radaelli, One-dimensional magnetic fluctuations in the spin-2 triangular lattice α -NaMnO₂, *Phys. Rev. Lett.* **103**, 077202 (2009).
- [30] F. K. K. Kirschner, R. D. Johnson, F. Lang, D. D. Khalyavin, P. Manuel, T. Lancaster, D. Prabhakaran, and S. J. Blundell, Spin Jahn-Teller antiferromagnetism in CoTi₂O₅, *Phys. Rev. B* **99**, 064403 (2019).
- [31] F. Lang, L. Jowitt, D. Prabhakaran, R. D. Johnson, and S. J. Blundell, FeTi₂O₅: A spin Jahn-Teller transition enhanced by cation substitution, *Phys. Rev. B* **100**, 094401 (2019).
- [32] V. Petricek, M. Dusek, and L. Palatinus, Crystallographic computing system JANA2006: General features, *Z. Kristallogr.* **229**, 345 (2014).
- [33] A. A. Coelho, *TopasAcademic: General Profile and Structure Analysis Software for Powder Diffraction Data* (Bruker AXS, Karlsruhe, Germany, 2012).

- [34] H.-H. Xu, Q.-Y. Liu, C. Xin, Q.-X. Shen, J. Luo, R. Zhou, J.-G. Cheng, J. Liu, L. L. Tao, Z.-G. Liu, M.-X. Huo, X.-J. Wang, and Y. Sui, Spin gap in quasi-one-dimensional $S = 3/2$ antiferromagnet, *Chin. Phys. B* **33**, 037505 (2024).
- [35] S. Wu, Y. Song, Y. He, A. Frano, M. Yi, X. Chen, H. Uchiyama, A. Alatas, A. H. Said, L. Wang, T. Wolf, C. Meingast, and R. J. Birgeneau, Short-range nematic fluctuations in $\text{Sr}_{1-x}\text{Na}_x\text{Fe}_2\text{As}_2$ superconductors, *Phys. Rev. Lett.* **126**, 107001 (2021).
- [36] M. Kauth, S. Rosenkranz, A. H. Said, K. M. Taddei, T. Wolf, and F. Weber, Soft elastic constants from phonon spectroscopy in hole-doped $\text{Ba}_{1-x}(\text{K}, \text{Na})_x\text{Fe}_2\text{As}_2$ and $\text{Sr}_{1-x}\text{Na}_x\text{Fe}_2\text{As}_2$, *Phys. Rev. B* **102**, 144526 (2020).
- [37] M. Loewenhaupt, B. D. Rainford, and F. Steglich, Dynamic Jahn-Teller effect in a rare-earth compound: CeAl_2 , *Phys. Rev. Lett.* **42**, 1709 (1979).
- [38] G. Güntherodt, A. Jayaraman, G. Batlogg, M. Croft, and E. Melczer, Raman scattering from coupled phonon and electronic crystal-field excitations in CeAl_2 , *Phys. Rev. Lett.* **51**, 2330 (1983).
- [39] P. Thalmeier and P. Fulde, Bound state between a crystal-field excitation and a phonon in CeAl_2 , *Phys. Rev. Lett.* **49**, 1588 (1982).
- [40] R. L. Melcher and B. A. Scott, Soft acoustic mode at the cooperative Jahn-Teller phase transition in DyVO_4 , *Phys. Rev. Lett.* **28**, 607 (1972).
- [41] E. Pytte, Structural phase transitions in spinels induced by the Jahn-Teller effect, *Phys. Rev. B* **3**, 3503 (1971).
- [42] E. Pytte, Dynamics of Jahn-Teller phase transitions, *Phys. Rev. B* **8**, 3954 (1973).
- [43] H. Liu and G. Khaliullin, Pseudo-Jahn-Teller effect and magnetoelastic coupling in spin-orbit Mott insulators, *Phys. Rev. Lett.* **122**, 057203 (2019).
- [44] T. Weber, B. Roessli, C. Stock, T. Keller, K. Schmalzl, F. Bourdarot, R. Georgii, R. A. Ewings, R. S. Perry, and P. Böni, Transverse acoustic phonon anomalies at intermediate wave vectors in MgV_2O_4 , *Phys. Rev. B* **96**, 184301 (2017).
- [45] H. Lane, P. M. Sarte, K. Guratinder, A. M. Arevalo-Lopez, R. S. Perry, E. C. Hunter, T. Weber, B. Roessli, A. Stunault, Y. Su, R. A. Ewings, S. D. Wilson, P. Böni, J. P. Attfield, and C. Stock, Spin-orbital correlations from complex orbital order in MgV_2O_4 , *Phys. Rev. Res.* **5**, 043146 (2023).
- [46] R. J. Birgeneau, J. K. Kjems, G. Shirane, and L. G. Van Uiter, Cooperative Jahn-Teller phase transition in PrAlO_3 , *Phys. Rev. B* **10**, 2512 (1974).
- [47] R. A. Cowley, Acoustic phonon instabilities and structural phase transitions, *Phys. Rev. B* **13**, 4877 (1976).
- [48] M. T. Dove, *Introduction to Lattice Dynamics* (Cambridge University Press, Cambridge, England, 1993).
- [49] A. A. Maradudin, Thermal expansion and phonon frequency shifts, *Phys. Status Solidi B* **2**, 1493 (1962).
- [50] K. Guratinder, E. Chan, E. E. Rodriguez, J. A. Rodriguez-Rivera, U. Stuhr, A. Stunault, R. Travers, M. A. Green, N. Qureshi, and C. Stock, Acoustic lattice instabilities at the magnetostructural transition in $\text{Fe}_{1.057(7)}\text{Te}$, *Phys. Rev. B* **108**, 214411 (2023).
- [51] S. L. Dudarev, G. A. Botton, S. Y. Savrasov, C. J. Humphreys, and A. P. Sutton, Electron-energy-loss spectra and the structural stability of nickel oxide: An LSDA + U study, *Phys. Rev. B* **57**, 1505 (1998).
- [52] A. I. Liechtenstein, V. I. Anisimov, and J. Zaanen, Density-functional theory and strong interactions: Orbital ordering in Mott-Hubbard insulators, *Phys. Rev. B* **52**, R5467 (1995).
- [53] P. A. Maksimov, A. V. Ushakov, Z. V. Pchelkina, Y. Li, S. M. Winter, and S. V. Streltsov, *Ab initio* guided minimal model for the “Kitaev” material $\text{BaCo}_2(\text{AsO}_4)_2$: Importance of direct hopping, third-neighbor exchange, and quantum fluctuations, *Phys. Rev. B* **106**, 165131 (2022).
- [54] S. V. Streltsov, A. S. Mylnikova, A. O. Shorikov, Z. V. Pchelkina, D. I. Khomskii, and V. I. Anisimov, Crystal-field splitting for low symmetry systems in *ab initio* calculations, *Phys. Rev. B* **71**, 245114 (2005).
- [55] D. Behr, L. S. Taran, D. G. Porter, A. Bombardi, D. Prabhakaran, S. V. Streltsov, and R. D. Johnson, Strain-induced antiferromagnetic domain switching via the spin Jahn-Teller effect, *Phys. Rev. B* **110**, L060408 (2024).
- [56] E. M. Stoudenmire, S. Trebst, and L. Balents, Quadrupolar correlations and spin freezing in $S = 1$ triangular lattice antiferromagnets, *Phys. Rev. B* **79**, 214436 (2009).
- [57] M. E. Valentine, T. Higo, Y. Nambu, D. Chaudhuri, J. Wen, C. Broholm, S. Nakatsuji, and N. Drichko, Impact of the lattice on magnetic properties and possible spin nematicity in the $S = 1$ triangular antiferromagnet NiGa_2S_4 , *Phys. Rev. Lett.* **125**, 197201 (2020).
- [58] H. Tsunetsugu and M. Arikawa, Spin nematic phase in $S = 1$ triangular antiferromagnets, *J. Phys. Soc. Jpn.* **75**, 083701 (2006).